Protein Tyrosine Phosphatase Epsilon Regulates Integrin-mediated Podosome Stability in Osteoclasts by Activating Src

Shira Granot-Attas,* Chen Luxenburg,†‡ Eynat Finkelshtein,* and Ari Elson*

Departments of *Molecular Genetics and †Molecular Cell Biology, The Weizmann Institute of Science, Rehovot 76100, Israel

The nonreceptor isoform of tyrosine phosphatase epsilon (cyt-PTPe) supports osteoclast adhesion and activity in vivo, leading to increased bone mass in female mice lacking PTPe (EKO mice). The structure and organization of the podosomal adhesion structures of EKO osteoclasts are abnormal; the molecular mechanism behind this is unknown. We show here that EKO podosomes are disorganized, unusually stable, and reorganize poorly in response to physical contact. Phosphorylation and activities of Src, Pyk2, and Rac are decreased and Rho activity is increased in EKO osteoclasts, suggesting that integrin signaling is defective in these cells. Integrin activation regulates cyt-PTPe by inducing Src-dependent phosphorylation of cyt-PTPe at Y638. This phosphorylation event is crucial because wild-type—but not Y638F—cyt-PTPe binds and further activates Src and restores normal stability to podosomes in EKO osteoclasts. Increasing Src activity or inhibiting Rho or its downstream effector Rho kinase in EKO osteoclasts rescues their podosomal stability phenotype, indicating that cyt-PTPe affects podosome stability by functioning upstream of these molecules. We conclude that cyt-PTPe participates in a feedback loop that ensures proper Src activation downstream of integrins, thus linking integrin signaling with Src activation and accurate organization and stability of podosomes in osteoclasts.

INTRODUCTION

Osteoclasts are large multinucleated cells of hematopoietic origin that degrade bone matrix. To perform this function osteoclasts must adhere firmly to bone using specialized adhesion structures called podosomes (Geiger *et al.*, 2001; Gimona and Buccione, 2006; Linder, 2007; Teitelbaum, 2007). Podosomes are punctate structures that contain an actin-rich core surrounded by a ring of associated proteins, which convey the signal generated by contact with matrix to the actin core and the actin cytoskeleton. Proteins present in the podosomal ring include integrins and associated molecules such as vinculin, paxillin, Cbl, Cas, Src, Pyk2, and the small GTPases Rho, Rac, and CDC42 (Linder and Aepfelbacher, 2003; Gimona, 2008).

In addition to osteoclasts podosomes are found in, among other cell types, macrophages, dendritic cells, and in endothelial and epithelial cells (Linder, 2007; Gimona *et al.*, 2008). In osteoclasts, however, the organization of podosomes is linked to the ability of the cell to fulfill its physiological role.

In cultured osteoclasts that are not actively resorbing bone, podosomes are scattered at random. Podosomes can assemble into clusters that grow and transform into dynamic rings, which further expand to form a large superstructure at the cell periphery that is characteristic of mature, bone-resorbing cells. In osteoclasts grown on degradable matrix, this peripheral, belt-like superstructure, referred to as the sealing zone, contains densely packed podosomes that are usually not individually discernible. In osteoclasts grown on nondegradable surface, podosomes are arranged in a less-crowded sealing zone-like structure (SZL), in which individual podosomes are visible (Destaing *et al.*, 2003; Luxenburg *et al.*, 2006a, 2007; Gimona *et al.*, 2008; Saltel *et al.*, 2008). Examination of osteoclast structure by scanning electron microscopy revealed that SZL podosomes are made of actin pillars and are interconnected by a dense array of radial actin fibers (Luxenburg *et al.*, 2007). Podosomes are dynamic and short-lived structures with an average life span of 1–5 min (Destaing *et al.*, 2003, 2008; Luxenburg *et al.*, 2006b). Interestingly, as podosomes become associated with rings and the SZL, which are structures typical of active resorption, their life span is reduced and they become further destabilized. The reason for this is not known (Luxenburg *et al.*, 2006a,b). Because osteoclast activity is dependent upon podosome-mediated adhesion to bone, pathways that regulate podosomal behavior are of importance in understanding how physiological bone resorption is regulated.

Tyrosine phosphorylation participates in osteoclast signaling pathways downstream of integrins, receptor activator of nuclear factor-κB ligand (RANKL) and macrophage colony-stimulating factor (M-CSF; CSF-1) (Bruzzaniti and Baron, 2006; Ross, 2006; Wada *et al.*, 2006), all of which play key roles in the differentiation and activity of osteoclasts. Disruptions in tyrosine phosphorylation can therefore significantly affect oste-

oclast activity in vivo. Accordingly, mice lacking Src contain increased amounts of dysfunctional osteoclasts that contain disorganized podosomes and exhibit significantly increased bone mass (Soriano *et al.*, 1991; Lowe *et al.*, 1993). The formation, structure, and life span of podosomes in osteoclasts is affected significantly by Src activity (Sanjay *et al.*, 2001; Miyazaki *et al.*, 2004; Luxenburg *et al.*, 2006b; Destaing *et al.*, 2008), although the noncatalytic domains of Src also seem important in this respect (Schwartzberg *et al.*, 1997; Destaing *et al.*, 2008). Aberrant podosomal organization, reduced osteoclast function, and increased bone mass also have been described in mice lacking Pyk2 or Syk (Gil-Henn *et al.*, 2007; Zou *et al.*, 2007).

In contrast to the tyrosine kinases, little is known about how tyrosine phosphatases (PTPs) regulate osteoclasts (Granot-Attas and Elson, 2008). The Src homology (SH)2 domain-containing PTP SHP1 inhibits osteoclast activity because mice lacking this phosphatase exhibit increased bone resorption and reduced bone mass (Aoki *et al.*, 1999; Umeda *et al.*, 1999). This effect may be due to SHP1 negatively regulating RANKL signaling in precursor cells (Zhang *et al.*, 2003). In contrast, the receptor-type PTP CD45 supports osteoclast activity; osteoclasts from CD45-deficient mice display aberrant morphology and reduced activity, which may be caused by reduced Src kinase activity in these cells (Shivtiel *et al.*, 2008). The receptor-type PTPRO (PTP-oc) is also believed to support osteoclast function by affecting Src activity (Amoui *et al.*, 2007). Targeted deletion of this phosphatase in RAW264.7 cells inhibited their osteoclastic differentiation in vitro, whereas osteoclast-directed overexpression of PTP-oc in transgenic mice increased bone resorption (Yang *et al.*, 2007; Sheng *et al.*, 2009). In vitro cell studies have suggested that PTP-PEST is an additional positive regulator of osteoclasts (Chellaiah and Schaller, 2009).

Another positive regulator of osteoclast activity is PTP epsilon (PTPe). Two major protein forms of PTPe exist—these are the receptor-type form (RPTPe) and the nonreceptor form (cyt-PTPe), which are produced by use of alternative promoters from the single *Ptpre* gene (Krueger *et al.*, 1990; Elson and Leder, 1995a,b; Tanuma *et al.*, 1999). The expression patterns of RPTPe and cyt-PTPe among cells and tissues are virtually nonoverlapping (Elson and Leder, 1995a); cyt-PTPe is expressed strongly in osteoclasts (Chiusaroli *et al.*, 2004) and is at the focus of this study. Our previous studies have shown that cyt-PTPe supports osteoclast activity by affecting the adherence of these cells to bone. Female mice lacking PTPe (EKO mice, which lack all forms of PTPe) exhibit increased bone mass and reduced osteoclast activity in vivo and in vitro, which coincides with reduced adhesion of these cells to bone in vivo (Chiusaroli *et al.*, 2004). EKO osteoclasts are also defective in recruiting hematopoietic precursor cells from the bone marrow into the general circulation (Kollet *et al.*, 2006). In agreement with the above-mentioned functional data, podosomes of osteoclast-like cells (OCLs) grown from bone marrow of EKO mice are typically disorganized and often lack a clear core-ring structure (Chiusaroli *et al.*, 2004). The present study broadens the scope of the abnormalities in the structure and dynamics of podosomes in EKO osteoclasts, and characterizes the molecular role of cyt-PTPe in osteoclasts and its regulation by physiological signaling.

MATERIALS AND METHODS

Reagents

The following mouse cDNAs used were used: cyt-PTPe and Y638F cyt-PTPe (Toledano-Katchalski and Elson, 1999), GFP cyt-PTPe (Kraut *et al.*, 2002). C277,572S cyt-PTPe was constructed from wild-type cyt-PTPe by site-directed mutagenesis followed by sequence verification. PTPe cDNAs were cloned in the pcDNA3 expression vector (Invitrogen, Carlsbad, CA) and contained a FLAG tag at their C termini. Also used were cDNAs for Chicken Y527F Src (a gift from Dr. S. Courtneidge, The Burnham Institute for Medical Research, La Jolla, CA), wild-type Src (from Dr. J. den Hertog, Netherlands Institute of Developmental Biology, Utrecht, The Netherlands), monomeric red fluorescent protein-labeled actin (from Dr. B. Geiger, The Weizmann Institute, Rehovot, Israel), and Pyk2 (from Dr. S. Lev, The Weizmann Institute). Polyclonal antibodies used included anti-PTPe (Elson and Leder, 1995b), anti-Y402 Pyk2 and anti-Y416 Src (Cell Signaling Technology, Danvers, MA), and anti phospho-PTPe. The latter antibody was shown previously to react specifically with PTPe phosphorylated at its C-terminal tyrosine residue (Y638 in cyt-PTPe=Y695 in RPTPe; Berman-Golan and Elson, 2007). Monoclonal antibodies used included anti-v-Src (clone 327; Calbiochem, San Diego, CA), anti-Pyk2 (clone 11; BD Biosciences, San Jose, CA), anti-phosphotyrosine (clone PY99; Santa Cruz Biotechnologies, Santa Cruz, CA), anti-Rho (BD Biosciences), and anti-Rac (Cytoskeleton, Denver, CO). Also used were anti-FLAG monoclonal antibodies coupled to agarose beads (clone M2; Sigma-Aldrich., St. Louis, MO). Actin was stained with phalloidin Alexa-488 (Invitrogen). PP1 and Y27632 were from Calbiochem. Adenoviruses for expressing red fluorescent protein (RFP) or Src were purchased from Capital Biosciences (Rockville, MD). Adenoviruses for expressing wild-type (WT) or Y638F cyt-PTPe were prepared by cloning the relevant mouse cDNAs into the viral genome by using the Adeno-1 system (Capital Biosciences). Cell-permeable C3 exoenzyme (a generous gift from Dr. Alexander Bershadsky of The Weizmann Institute) was from Cytoskeleton.

Mice

Gene targeted mice lacking all forms of PTPe (EKO mice, C57BL/6 × 129 genetic background) were described previously (Peretz *et al.*, 2000). Mice transgenic for an actin-green fluorescent protein (GFP) fusion protein were kindly provided by Dr. Andrew Matus (Friedrich Miescher Institute, Basel, Switzerland) (Fischer *et al.*, 2000) and were crossed with EKO mice. All experiments were approved by the Institutional Animal Care and Use Committee of The Weizmann Institute in accordance with Israeli law.

Cell Culture

Osteoclasts: Marrow was extracted from femora and tibiae of 5- to 10-wk-old mice. Bone marrow cells were cultured in OCL medium (α-minimal essential medium; Sigma-Aldrich) containing 10% fetal calf serum (FCS; Invitrogen), 4 mM glutamine, 50 U/ml penicillin, 50 μg/ml streptomycin, 20 ng/ml M-CSF, and 20 ng/ml RANKL (both from R&D Systems, Minneapolis, MN)). Cells were incubated at 37°C and 5% CO_2 for 5–6 d. RAW264.7 cells were purchased from the American Type Culture Collection (Manassas, VA) and grown in complete DMEM medium (Invitrogen) supplemented with 10% FCS (HyClone Laboratories, Logan, UT), glutamine, and antibiotics as described above, at 37°C and 7% CO_2. RAW264.7 cells express negligible amounts of endogenous PTPe (data not shown). Cells were differentiated in OCL medium as described above at 37°C in 5% CO_2 for 4 d. Chinese hamster ovary (CHO) cells stably expressing the $\beta3$ integrin subunit (CHO$\beta3$ cells; a generous gift from Dr. M. Ginsberg, University of California, San Diego, La Jolla, CA) were grown in Ham's-F12 medium (Biological Industries, Beit Haemek, Israel) supplemented with 10% FCS (Invitrogen), glutamine, and antibiotics as described above. SYF cells were maintained as described in Gil-Henn and Elson (2003). RAW264.7 and CHO$\beta3$ cells were transfected using Lipofectamine 2000 or Lipofectamine (Invitrogen), respectively, according to the manufacturer's instructions.

Replating Experiments

After overnight starvation in medium containing 0.1% FCS, CHO$\beta3$ cells were trypsinized, suspended in DMEM containing 20 mM HEPES, and 1 mg/ml bovine serum albumin, and incubated at 37°C for an hour with gentle rotation. RAW264.7 preosteoclasts and primary bone marrow preosteoclasts were starved on their third and fourth days of differentiation, respectively, for 4 h in OCL medium containing 1% serum and no cytokines. Cells were detached by a short treatment with 10 mM EDTA and incubated as described above. In some cases, cells were replated on plates precoated with 20 μg/ml fibronectin (Sigma-Aldrich), 10 μg/ml vitronectin (Biological Industries), 10% serum, or 20 mg/ml poly-L-lysine. For replating of mature primary OCLs, bone marrow cells were induced to differentiate on plastic dishes covered with rat tail collagen gel (Roche, Basel, Switzerland) for 5 d. The collagen gel was digested with 0.1% collagenase (Sigma-Aldrich) at 37°C for 20 min with gentle shaking, after which the cells were replated on glass slides and fixed for analysis.

Adenoviral Infection of OCLs

Bone marrow from mice was cultured in OCL medium as described above in 35-mm glass-bottomed tissue culture plates (3–4 plates/mouse). Three days after seeding, medium was replaced with 1 ml of OCL medium containing adeno-RFP or a mixture of adeno-RFP and adenoviruses for expression Src or cyt-PTPe (WT or Y638F). After overnight incubation the medium was changed and the cells were fed daily with fresh OCL medium (containing

cytokines). Cells were processed for live-cell imaging 6–8 d after seeding. Most cells in these cultures were infected and expressed RFP.

Immunoprecipitation, Src Activity, and Protein Blotting

FLAG-tagged WT and Y638F cyt-PTPe were expressed in 293 cells and purified by immunoprecipitation with anti-FLAG antibodies as described previously (Tiran *et al.*, 2006). The purity and amounts of eluted material were determined by gel electrophoresis and silver staining. For pull-down of Src and Pyk2 with cyt-PTPe, 2 mg of cell lysates were incubated with 5 μg of purified WT or Y638F cyt-PTPe bound to M2 FLAG beads for 1 h. The PTP inhibitor sodium iodoacetate (5 mM) was present during all stages of this study, including the initial precipitation of FLAG-PTPe. Src kinase activity assay was performed as described previously (Gil-Henn and Elson, 2003) by allowing precipitated Src to phosphorylate enolase with [γ-^{32}P]ATP. SDS-polyacrylamide gel electrophoresis (PAGE), blotting, and antibody hybridization were done as described previously (Gil-Henn *et al.*, 2000).

Rac and Rho Activity Assays

Activities were determined using the RhoA and Rac1 Activation Assay Biochem kits (Cytoskeleton) according to manufacturer's instructions. In brief, 2 mg of total protein from lysates of primary OCLs from bone marrow were used to pull down guanosine triphosphate (GTP)-bound Rac or Rho. Amounts of activated, precipitated Rac/Rho were determined by protein blotting with antibodies against Rac or Rho, followed by normalizing to total Rac/Rho amounts detected in the crude lysates.

Fluorescence Microscopy and Live-Cell Imaging

Cells were fixed for 2 min in warm 3% paraformaldehyde (PFA) (Merck, Darmstadt, Germany) containing 0.5% Triton X-100 (Sigma-Aldrich) and then in 3% PFA alone for an additional 20 min. After incubations with primary and secondary antibodies, cells were mounted with Fluoromount-G solution (Southern Biotechnology Associates, Birmingham, AL). Images were collected on a confocal Radiance 2100 laser scanning system (Bio-Rad Laboratories, Hercules, CA) or on a deconvolution DeltaVision system (Applied Precision, Issaquah, WA), including an inverted microscope (IX70) equipped with a UPlanSApo 100×/1.4 numerical aperture objective (Olympus, Tokyo, Japan). Images were acquired and deconvoluted using Resolve3D software (Applied Precision). The latter system was also used for live-cell imaging, in which cells were examined in glass-bottomed plates in a temperature- and atmosphere-controlled chamber. Cells were examined in DMEM containing 25 mM HEPES (Biological Industries) and 10% FCS. Life spans of podosomes were measured by following individual podosomes in consecutive images of cells as described in Luxenburg *et al.* (2006b). After adenoviral infection, only infected (RFP-expressing) cells were analyzed.

Scanning Electron Microscopy

Osteoclasts were prepared using the ventral membrane preparation (VMP) technique as described in Luxenburg *et al.* (2007). In brief, bone marrow cells were cultured on electron microscope grids and induced to differentiate into mature osteoclasts. The osteoclast cell body was mechanically removed by short incubation in hypotonic solution followed by mechanical peeling of the cells. The samples were processed for electron microscopy and visualized using the Ultra 55 high-resolution scanning electron microscope system (Carl Zeiss, Oberkochen, Germany).

Statistical Analysis

Except where noted, statistical analysis was performed by a two-tailed, unpaired Student's *t* test, with the significance level set at p = 0.05.

RESULTS

Cyt-PTPe Is Required for Proper Structure, Stability, and Dynamics of Podosomes

Previous studies have shown that podosomes are arranged abnormally in OCLs from EKO mice. In particular, the fraction of OCLs whose podosomes are arranged in a SZL at the cell periphery, which is typical of resorbing cells, is reduced 10-fold in EKO OCLs (Chiusaroli *et al.*, 2004). To study podosomal structures in greater detail, we examined OCLs by scanning electron microscopy. In agreement with previous studies (Luxenburg *et al.*, 2007), podosomes in the SZL of OCLs from WT mice occurred as individual, evenly distributed concentrations of actin that were interconnected by a radial network of fine actin filaments (Figure 1, A and B). In contrast, the periphery of EKO OCLs contained a complex network of disorganized fibers with very few podosomal
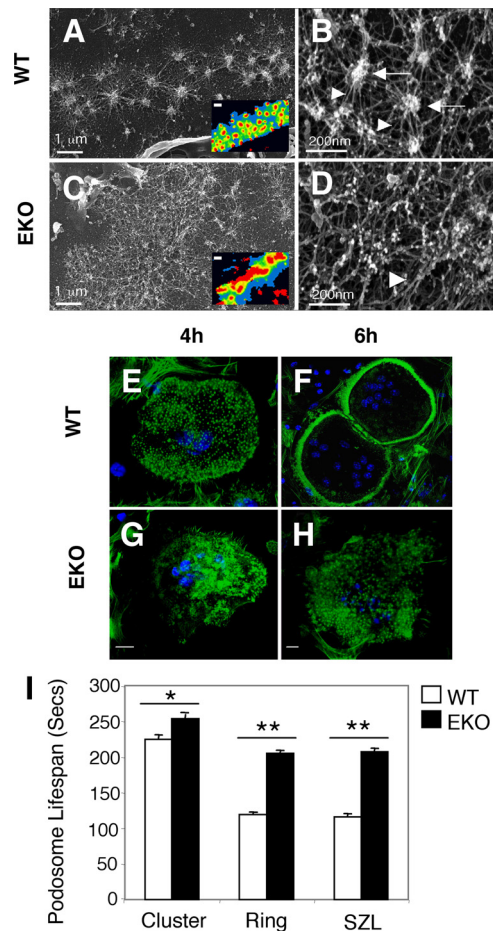

Figure 1. Lack of PTPe disrupts podosomal structure and dynamics. (A–D) Lack of PTPe disrupts podosomal structure. Ventral membranes from wild-type (WT; A and B) or PTPe-deficient (EKO; C and D) primary OCLs were examined by high-resolution scanning electron microscopy. The SZL of WT cells contains punctate podosomal cores (arrows; B) interconnected by actin fibers (arrowheads; B) (Luxenburg *et al.*, 2007); EKO cells do not contain visible cores (D). Insets in A and C show the SZL of intact OCLs stained for actin (red) and vinculin (blue), similar to (Chiusaroli *et al.*, 2004). Bars, 1 μm (A and C) and 0.2 μm (B and D) or 5 μm (insets in A and C). (E–H) EKO OCLs do not organize their podosomes well after replating. OCLs were differentiated from bone marrow of WT or EKO mice in collagen gels, lifted, replated onto glass slides, stained for actin (green) and DNA (blue) at the indicated time points after plating, and analyzed by confocal microscopy. Pictures shown are representative of the WT (E and F) versus EKO (G and H) cultures. Bars, 10 μm. (I) Lack of PTPe increases podosomal stability. WT and EKO OCLs prepared from actin-GFP mice were grown on glass and examined by live-cell imaging. Shown is the average time between appearance and disappearance of individual GFP-labeled actin podosomal cores. N = 203–317 individual podosomes from seven to eight different cells per bar. *p = 0.00095, **p < 1 × 10^{-6}. See numerical data in Supplemental Table 1.

structures (Figure 1, C and D). Qualitatively similar observations were made when OCLs were analyzed by immunostaining for the podosomal core protein actin and for vinculin, which normally surrounds the actin-rich core. Podosomal cores in the SZL of WT OCLs were of similar size and regular distribution and were surrounded by a uniform vinculin-rich region (Figure 1A, inset). In contrast, the SZL of OCLs from PTPe-deficient mice was severely disorganized and contained large irregular concentrations of actin

(Figure 1C, inset; also see Chiusaroli *et al.*, 2004). We conclude that loss of cyt-PTPe severely disrupts the internal structure of podosomes in the SZL.

Podosomes of EKO OCLs are abnormal also in their dynamics. When mature differentiated OCLs from WT mice were lifted and replated on glass slides in the presence of serum, individual podosomes were visible after 3 h. Four hours after plating podosomes began to arrange into clusters, and after 6 h many cells contained the typical SZL peripheral array of podosomes (Figure 1, E and F). In contrast, individual podosomes occurred with delay in EKO OCLs and most did not proceed to form an SZL (Figure 1, G and H). These results agree with previous studies, in which the fraction of cells that eventually contained a SZL was 35.5 ± 2.6% (mean ± SE) in WT cells versus 3.2 ± 1.4% in EKO cells (Chiusaroli *et al.*, 2004). Podosomes in EKO OCLs are therefore unable to organize properly in response to an acute stimulus in the form of replating.

Podosomes are short-lived structures, whose life span is further shortened upon associating with structures typical of active osteoclasts, such as rings or the SZL (Luxenburg *et al.*, 2006b). To determine whether lack of cyt-PTPe affects podosomal life span, we examined OCLs from WT or EKO mice that expressed an actin-GFP transgene that fluorescently labeled their podosomal cores. The time that elapsed between appearance and disappearance of individual cores in these cells was measured using live-cell imaging. Our results confirm that in WT OCLs the life span of podosomal cores that are arranged in clusters, which are typical of nonresorbing cells, is significantly longer than cores arranged in rings or in the SZL. In contrast, the life span of podosomal cores from EKO OCLs is significantly longer irrespective of their organization within the cells; this is especially noticeable in the rings and the SZL (Figure 1I and Supplemental Table 1). We conclude that cyt-PTPe participates in regulating podosomal structure and function in OCLs, and that lack of this phosphatase affects the internal structure, stability, and cellular organization of podosomes.

Dysregulation of Src, Pyk2, Rho, and Rac in OCLs That Lack cyt-PTPe

The structure and organization of podosomes in OCLs are regulated by integrin-mediated mechanical contact with matrix. Major effectors of integrin signaling in OCLs include the tyrosine kinases Src and Pyk2 and their downstream effectors, such as the small GTPases Rho and Rac (Fukuda *et al.*, 2005; Jurdic *et al.*, 2006). Examination of EKO OCLs indicated that the kinase activity of Src was reduced by ~40% (Figure 2A). In agreement, autophosphorylation of Src at Y416, which qualitatively correlates with Src activity, was reduced to a greater extent. Autophosphorylation of Pyk2 at Y402, which roughly correlates with activity of this kinase, was reduced as well in EKO osteoclasts (Figure 2B). In separate experiments, we precipitated the active forms of Rho and Rac by using glutathione transferase (GST) fusion proteins that bound the GTP-bound forms of these GTPases. EKO OCLs exhibited a doubling in activated Rho and a drop of 39% in activated Rac (Figures 2, C and D). The studies presented here were performed in relatively pure and homogeneous cultures of OCLs differentiated from bone marrow by using purified M-CSF and RANKL. Previous studies used EKO OCLs produced by coculturing bone marrow with WT osteoblasts. The less-homogeneous nature of these cultures and partial contamination by osteoblasts may have masked the differences in Src and Pyk2, which were not detected previously. In all, the data indicate that lack of
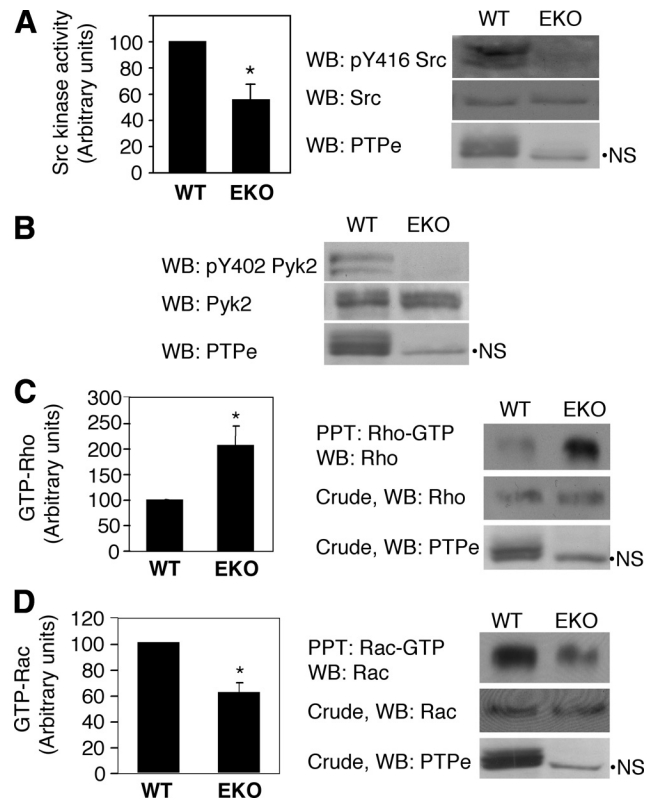

Figure 2. Altered activities of Src, Pyk2, Rho, and Rac in EKO OCLs. (A) Left, Src was precipitated from primary WT or EKO OCLs and its activity was assayed in vitro; Src activity from EKO OCLs was 58.9 ± 12.7% of WT, N = 4, p = 0.018 by paired Student's *t* test. Right, autophosphorylation of Src at Y416 is reduced in lysates of primary EKO OCLs. NS, nonspecific band. (B) Phosphorylation of Pyk2 is reduced at Y402 in EKO OCLs. (C). Lysates of primary OCLs prepared from bone marrow of WT or EKO mice were subjected to a pull-down assay using the Rho binding domain of Rhotekin fused to GST. Left, amounts of active (GTP-bound) Rho are increased by 107 ± 37% in EKO cells relative to WT (mean ± SE, normalized to Rho expression levels in each sample; *p = 0.045, by paired two-tailed Student's *t* test; N = 4). Right, representative protein blot depicting levels of Rho-GTP (top), total Rho (middle), and cyt-PTPe (bottom). (D) Similar to C, using a GST fusion of the p21 activated kinase 1 (PAK1) to pull down GTP-bound Rac. GTP-Rac is decreased by 39 ± 8% in EKO relative to WT cells (*p = 0.041, by paired two-tailed Student's *t* test; N = 3). NS, nonspecific band.

cyt-PTPe strongly affects the activity of molecular effectors of integrin signaling in OCLs.

Integrin Activation Induces C-terminal Phosphorylation of PTPe

To examine the molecular role of cyt-PTPe in regulating podosomes, we first examined the subcellular localization of this phosphatase. Because existing anti-PTPe antibodies do not function well in immunostaining studies, we expressed green fluorescent protein (GFP)-tagged cyt-PTPe in RAW264.7 cells, a mouse hematopoietic cell line that can be differentiated into matrix-degrading OCLs with M-CSF and RANKL. cyt-PTPe was expressed throughout the cell, including in a prominent peripheral ring that overlapped in part with the podosomes of the SZL, which were visualized by labeling with RFP-actin (Figure 3, A–C and G). In contrast, GFP itself did not localize significantly to the cell periphery (Figure 3, D–F and H). Cyt-PTPe is therefore present throughout the
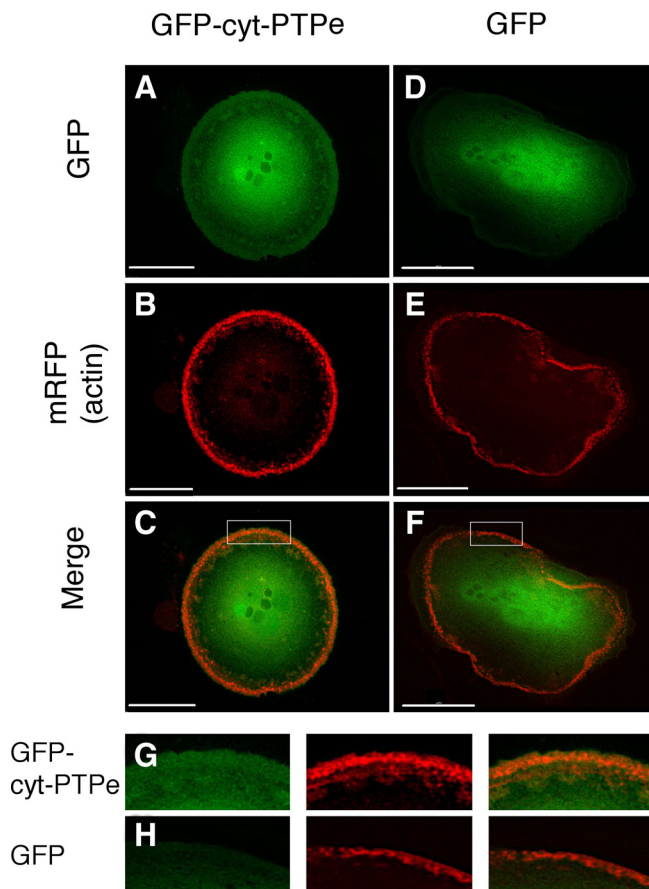
GFP-cyt-PTPe   GFP

Figure 3. cyt-PTPe is found near podosomes. RAW264.7 cells were cotransfected with actin-monomeric RFP and either cyt-PTPe-GFP (A–C) or GFP alone (D–F), allowed to differentiate on glass slides into OCLs, and examined with a Delta Vision deconvolution fluorescence microscope. G and H depict higher magnification of the regions indicated in C and F, respectively. Note the significantly weaker GFP staining at the cell periphery, but not center, in D versus A. Bars, 30 μm.

Figure 4. Integrin activation induces C-terminal phosphorylation of PTPe. (A) WT or Y638F cyt-PTPe were expressed in CHOβ3 cells. Cells were grown on plastic plates (A), serum-starved, lifted, and maintained in suspension for 60 min (S), and then plated on plates coated with fibronectin (FN) or poly-L-lysine (PL) for 10 min. After lysis, PTPe was precipitated and analyzed for phospho-tyrosine content by protein blotting with a general anti-p-tyrosine antibody. (B) Similar to A except that PTPe was expressed in RAW264.7 OCLs and phosphorylation of PTPe was examined using an anti C-terminal phospho-PTPe antibody (Berman-Golan and Elson, 2007). Cells were plated on vitronectin (Vn)-coated plates for 30 min. (C) Similar to B, using primary mouse OCLs differentiated from bone marrow of WT mice. (D) Similar to A, using CHOβ3 cells expressing the receptor-type form of PTPe, RPTPe, and its C-terminal Y-to-F mutant Y695 RPTPe. Y695 in RPTPe is identical to Y638 in cyt-PTPe. Mass markers are in kilodaltons.

OCL, including in the vicinity of podosomes; its precise structural association with podosomes requires further study. We note that several proteins that play key roles in podosomal function, such as Src itself (Tanaka *et al.*, 1996), are not localized exclusively to podosomes in OCLs.

Data presented thus far suggests that cyt-PTPe may regulate integrin signaling in osteoclasts. Previous studies have indicated that C-terminal phosphorylation of PTPe (at Y638 in cyt-PTPe=Y695 in the receptor isoform RPTPe) is an important regulator of the physiological role of the phosphatase. Phosphorylation enables RPTPe to activate Src in mammary tumors (Berman-Golan and Elson, 2007) and promotes inhibitory association of cyt-PTPe with microtubules (Sines *et al.*, 2007). To determine whether integrin signaling affects phosphorylation of cyt-PTPe at Y638, we examined CHOβ3 cells, which express endogenous αv and exogenous β3 integrin subunits; αvβ3 integrin is the major functional integrin in osteoclasts. Exogenous cyt-PTPe was phosphorylated in adherent CHOβ3 cells, was not phosphorylated in cells held in suspension, and was rephosphorylated in cells replated on dishes coated with the integrin ligand fibronectin (Figure 4A). cyt-PTPe was not phosphorylated in cells that were replated on plates coated with polylysine, indicating that it is phosphorylated in response to constitutive or acute activation of integrins. Y638F cyt-PTPe was not phos-
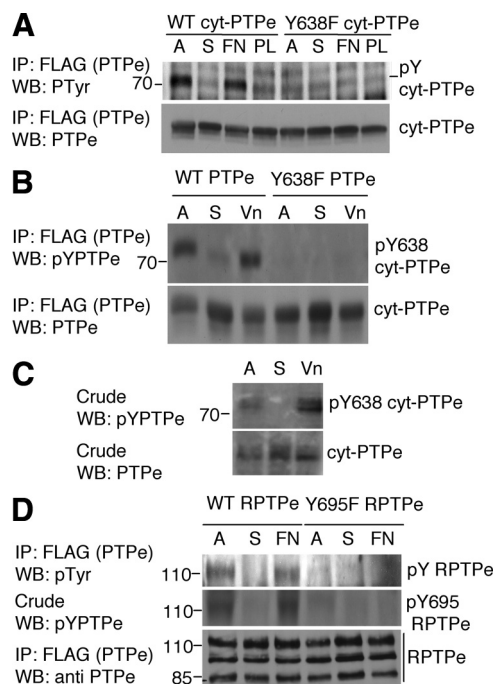
phorylated in adherent or in replated CHOβ3 cells (Figure 4A), indicating that integrin activation induces phosphorylation of cyt-PTPe exclusively at Y638. Immunofluorescence studies indicated that the subcellular distribution patterns of Y638F and of WT cyt-PTPe are identical (data not shown); hence, lack of phosphorylation of Y638F cyt-PTPe was not due to its mislocalization. Similar adhesion-linked phosphorylation of cyt-PTPe at Y638 was observed when the phosphatase was examined in RAW264.7 OCLs plated on the integrin ligand vitronectin (Figure 4B), by using an antibody specific for C-terminally phosphorylated PTPe. Most importantly, similar phosphorylation at Y638 was observed when endogenous cyt-PTPe was examined in primary WT OCLs (Figure 4C), indicating that phosphorylation of cyt-PTPe at Y638 is triggered by integrins also in vivo. Adhesion-dependent phosphorylation of the same C-terminal tyrosine residue was observed also in the receptor-type RPTPe (Figure 4D), suggesting that this form, which is absent from OCLs, may participate in integrin signaling in other cell types.

Activities of Src and cyt-PTPe Are Required for Integrin-Mediated Phosphorylation of cyt-PTPe

The major tyrosine kinases downstream of integrins in osteoclasts are Src and Pyk2. To determine whether either
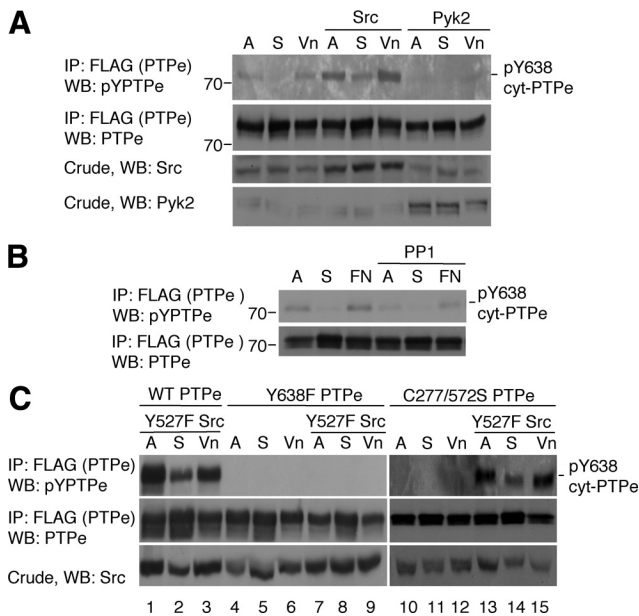
Figure 5. Src induces phosphorylation of cyt-PTPe after integrin activation. (A) WT FLAG-tagged cyt-PTPe was expressed in RAW264.7 OCLs along with Src or Pyk2. Lifting and replating of the cells and analysis of cyt-PTPe phosphorylation were performed as in Figure 4B. (B) WT cyt-PTPe was expressed in CHOβ3 cells. Cells were treated with 10 μM PP1 for 30 min as indicated and analyzed as in Figure 4A. (C) WT, Y638F, or C277/572S cyt-PTPe were expressed in RAW264.7 OCLs with constitutively active Y527F Src as indicated. Cells were treated and analyzed as in Figure 4B. In all panels, A, adherent cells; S, suspended cells; Vn, replated on vitronectin; and FN, replated on fibronectin. Mass markers are in kilodaltons.

kinase affects phosphorylation of cyt-PTPe, we expressed cyt-PTPe together with Src or Pyk2 in RAW264.7 OCLs. As before, cyt-PTPe was phosphorylated at Y638 in adherent cells and in cells replated on vitronectin (Figure 5A). Expression of wild-type Src, but not of Pyk2, significantly increased phosphorylation of cyt-PTPe, suggesting that phosphorylation is regulated by Src (Figure 5A). In agreement, phosphorylation of cyt-PTPe at Y638 was significantly reduced in RAW 264.7 OCLs after treatment with the Src family kinase inhibitor PP1 (Figure 5B). PP1 did not completely prevent phosphorylation of cyt-PTPe despite preventing phosphorylation of Shc in the same cells (data not shown), suggesting that Src is probably not the only kinase that regulates phosphorylation of cyt-PTPe downstream of activated integrins. Of note, phosphorylation of cyt-PTPe downstream of Src does not occur in 293 cells (Berman-Golan and Elson, 2007), raising the possibility that it might be indirect or require the presence of a third molecule.

As expected, expressing constitutively active (Y527F) Src in RAW264.7 cells increased phosphorylation of WT cyt-PTPe at Y638 but did not affect Y638F cyt-PTPe (Figure 5C, lanes 1–9). Interestingly, catalytically inactive, substrate-trapping (Flint *et al.*, 1997) (C277,572S) cyt-PTPe (CCSS cyt-PTPe) was not phosphorylated (Figure 5C, lanes 10–12), suggesting that catalytic activity of cyt-PTPe is needed for its own phosphorylation. Similar results were obtained with another inactive trapping mutant of cyt-PTPe, D245A cyt-PTPe (data not shown). Y527F Src did induce phosphorylation of CCSS cyt-PTPe at Y638 (Figure 5C, lanes 13–15), indicating that lack of phosphorylation of CCSS cyt-PTPe is not due to inaccessibility of Y638 due to aberrant folding of

CCSS cyt-PTPe or its possible interactions with other molecules. Increasing Src activity can then overcome the requirement for active cyt-PTPe for phosphorylation of the phosphatase.

C-Terminal Phosphorylation Is Required for cyt-PTPe to Activate Src, to Associate with Src and Pyk2, and to Shorten Podosomal Life Span in OCLs

Src is a known substrate of PTPe in mammary tumor cells and in fibroblasts; the phosphatase activates Src by removing its inhibitory phosphorylation at Y527 (Gil-Henn and Elson, 2003). Decreased Src activity in EKO OCLs (Figure 2A) and the ability of constitutively active Src to bypass the need for active cyt-PTPe in PTPe phosphorylation (Figure 5C) suggest that PTPe activates Src in OCLs as well. To investigate this possibility, we expressed wild-type cyt-PTPe in OCLs from EKO mice by adenoviral infection. The non-phosphorylatable Y638F cyt-PTPe was also included in this study to examine the functional effects of phosphorylation at this site; expression levels of both forms of cyt-PTPe were similar to those of endogenous cyt-PTPe in WT OCLs (Figure 6A). Endogenous Src exhibited basal activity in EKO OCLs in the absence of cyt-PTPe due to its partial activation by other PTPs. Src activity was increased more than twofold upon expression of WT cyt-PTPe (Figure 6B); in contrast, expression of Y638F resulted in a trend for increased Src activity relative to mock-infected cells, which did not reach statistical significance (Figure 6B). As indicated previously, this result is not due to mislocalization of the Y638F cyt-PTPe protein. Similar changes in Src activity were observed when exogenous WT and Y638F cyt-PTPe were expressed in RAW264.7 OCLs (Figure 6, C and D). Src activity in RAW264.7 cells held in suspension was inconsistent between experiments (data not shown), most likely the result of dysregulation of multiple processes that regulate Src activity in these normally adherent cells. Src activity returned to its normal values (including its dependence on phosphorylation of cyt-PTPe; Figure 4C) in readherent cells, a finding that is consistent with these effects being influenced by integrin-mediated cell adhesion. Further studies revealed that upon its addition to lysates of primary mouse OCLs, WT cyt-PTPe formed stable complexes with Src and Pyk2. In contrast, Y638F cyt-PTPe did not associate with either kinase (Figure 6E).

To understand further the role of cyt-PTPe and of its phosphorylation in OCLs we examined podosomal stability in the SZL of EKO OCLs, in which we expressed wild-type cyt-PTPe or its Y638F mutant. As in Figure 1I, these studies used OCLs that expressed a transgenic actin-GFP fusion protein, which allowed following podosomal cores by live-cell imaging. As observed previously in this study, podosomal cores found in the SZL of EKO OCLs were significantly longer lived than their counterparts from WT cells (Figure 6F and Supplemental Table 2). Expression of WT cyt-PTPe in EKO OCLs shortened the life span of their SZL podosomal cores to values observed in the SZL of WT OCLs. In contrast, expression of Y638F cyt-PTPe in EKO OCLs resulted in a trend for shortened podosomal life span that did not reach statistical significance (Figure 6F and Supplemental Table 2). In all, we conclude that cyt-PTPe associates with Src and activates this kinase in OCLs; cyt-PTPe is also required for maintaining the relatively short life span of podosomal cores in these cells. Phosphorylation of cyt-PTPe at Y638 is a critical physiological regulatory mechanism of this phosphatase in these respects, because Y638F cyt-PTPe, which cannot be phosphorylated at this site, cannot perform these roles.
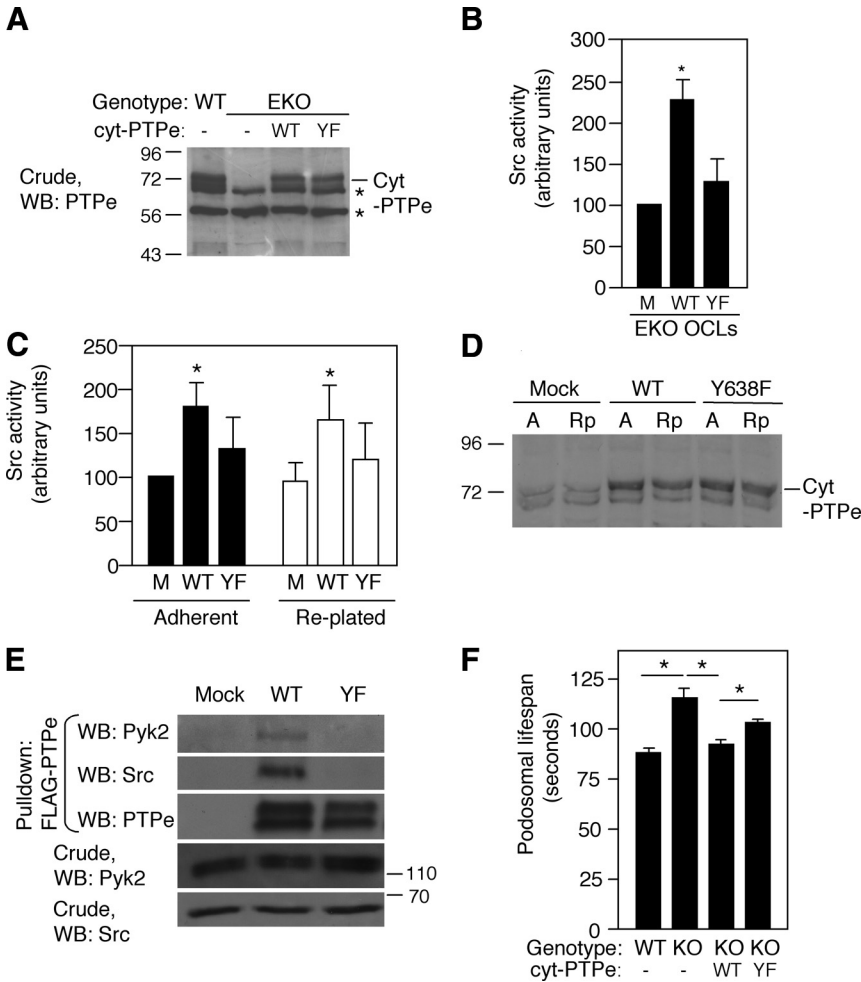
A

Genotype: WT   EKO

cyt-PTPe: -   -   WT   YF

Crude,
WB: PTPe

96 —
72 —
56 —
43 —

} Cyt
* -PTPe
*

B

Src activity (arbitrary units)

300 / 250 / 200 / 150 / 100 / 50 / 0

M   WT   YF

EKO OCLs

C

Src activity (arbitrary units)

250 / 200 / 150 / 100 / 50 / 0

M WT YF   M WT YF

Adherent   Re-plated

D

Mock   WT   Y638F

A   Rp   A   Rp   A   Rp

96 —
72 —

—Cyt -PTPe

E

Mock   WT   YF

Pulldown: FLAG-PTPe

WB: Pyk2

WB: Src

WB: PTPe

Crude, WB: Pyk2   —110

Crude, WB: Src   —70

F

Podosomal lifespan (seconds)

125 / 100 / 75 / 50 / 25 / 0

Genotype: WT   KO   KO   KO
cyt-PTPe: -   -   WT   YF

Figure 6. cyt-PTPe activates Src, associates with Src and Pyk2, and shortens podosomal life span in a phosphorylation-dependent manner. (A) WT or Y638F (YF) cyt-PTPe were expressed by adenoviral infection in OCLs differentiated from bone marrow of EKO mice. Blot shows expression of endogenous cyt-PTPe in WT OCLs and expression of exogenous cyt-PTPe in EKO cells. *, nonspecific bands. (B). Activity of endogenous Src was analyzed in EKO OCLs expressing WT or Y638F cyt-PTPe. Care was taken to analyze cultures in which expression of WT and of Y638F cyt-PTPe was similar, as in A. M, mock-infected control cells. Activity of Src was increased in the presence of WT or Y638F cyt-PTPe to 230 ± 35% or to 130 ± 28%, respectively, relative to mock-infected cells (mean ± SE; normalized to Src expression in each sample. *p = 0.026 by paired, two-tailed Student's *t* test. N = 5). (C) Expression of cyt-PTPe in RAW264.7 cells activates Src. WT or Y638F (YF) cyt-PTPe was expressed at similar levels in RAW264.7 cells, which were then differentiated with M-CSF and RANKL. Cells were analyzed either adherent or 10 min after replating. Activity of Src was increased in the presence of WT cyt-PTPe to 178 ± 24% relative to mock-transfected cells (M). *p ≤ 0.04, by paired two-tailed Student's *t* test; N = 7. (D) Expression of endogenous cyt-PTPe (Mock) or of exogenous (+ endogenous) cyt-PTPe (WT, Y638F lanes) in adherent (A) or replated (Rp) RAW264.7 cells. *, nonspecific bands. (E) WT, but not Y638F, cyt-PTPe associates with Src and Pyk2 in OCLs. Crude lysates of primary OCLs from WT mice were subjected to an in vitro pull-down assay using purified FLAG-tagged WT or Y638F cyt-PTPe. Mass markers are in kilodaltons. (F). WT, but not Y638F, cyt-PTPe shortens the life span of SZL podosomes from EKO OCLs. WT and EKO OCLs prepared from actin-GFP mice were grown on glass, infected with adenoviral vectors expressing WT or Y638F cyt-PTPe, and examined by live-cell imaging. All four cultures were also infected with adenovirus-RFP to identify infected cells. Shown is the average time between appearance and disappearance of individual GFP-labeled actin podosomal cores. *, p ≤ 3.4 × 10^{-6}, N = 79–346 podosomes from two to four distinct cells per bar. See numerical data in Supplemental Table 2.

cyt-PTPe Controls Podosomal Stability in OCLs by Regulating Src and Rho

Absence of cyt-PTPe from OCLs stabilizes podosomes in correlation with reduced Src activity (Figures 1I and 2A), whereas expressing cyt-PTPe in EKO OCLs destabilizes podosomes and increases Src activity (Figure 6). Together with previous reports that reduced activity of Src lengthens podosomal life span (Luxenburg *et al.*, 2006b; Destaing *et al.*, 2008), these results suggest a causative link between these events, namely that lack of cyt-PTPe stabilizes podosomes by reducing Src activity. According to this mechanism increasing Src activity in EKO OCLs should shorten the life span of podosomes, thus correcting the aberrant podosomal life span phenotype of these cells. To examine this possibility, we used adenoviral vectors to express WT Src in OCLs prepared from WT or EKO mice that carried the actin-GFP transgene; podosomal stability in the SZL was examined by live-cell imaging. In agreement with results presented in Figures 1 and 6, podosomes from EKO OCLs that were not infected with Src adenovirus were more stable than their counterparts from WT cells (Figure 7). Added expression of Src in WT and EKO OCLs shortened significantly the life spans of podosomes; the differences in podosomal life span

between the two genotypes disappeared (Figure 7 and Supplemental Table 3). Addition of Src therefore corrects the podosome stability phenotype of EKO OCLs, strongly supporting the conclusion that this phenotype is caused by reduced biological activity of Src that is, in turn, caused by loss of cyt-PTPe.

The small GTPase Rho is a known downstream effector of integrins and of Src in regulating podosome distribution in OCLs (Jurdic *et al.*, 2006; Ory *et al.*, 2008). Rho activity is doubled in EKO OCLs (Figure 2C), suggesting that increased Rho activity contributes to increased podosome stability in the absence of cyt-PTPe. To examine this possibility, we determined whether inhibition of Rho or of Rho kinase (ROCK), a downstream effector of Rho, would shorten podosome life span in the SZL of EKO OCLs. WT and EKO OCLs were treated with cell-permeable C3 exoenzyme, an inhibitor of Rho, or with the ROCK inhibitor Y27632, and SZL podosomes were examined using live-cell imaging. Inhibition of Rho by the C3 exoenzyme significantly shortened podosomal life span in both WT and EKO OCLs (Figure 7 and Supplemental Table 3). Inhibition of ROCK had little effect on WT OCLs, but significantly shortened the life span of podosomes in the SZL of EKO OCLs to levels similar to
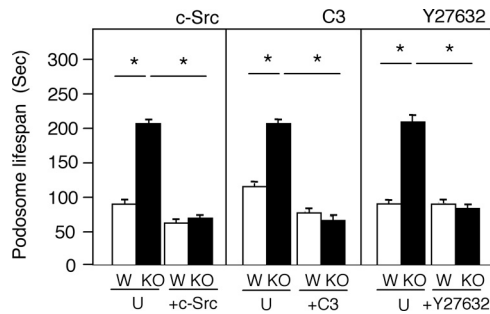
Figure 7. The abnormally long life spans of SZL podosomes in EKO OCLs are shortened by correcting abnormalities in Src or in downstream signaling elements. Left, WT (W) and EKO (KO) primary OCLs expressing an actin-GFP transgene were infected (+c-Src) or not (U) with adenovirus containing Src. Cells were coinfected with adeno-RFP to allow identification of infected cells. The life spans of the GFP-labeled podosome cores of these cells were measured by live-cell imaging. Middle, similar to left, except that cells were treated (+C3) or not (U) with 2 μg/ml cell-permeable C3 exoenzyme for 4 h and were not infected with adeno-RFP. Right, similar to middle, except that cells were treated or not with 10 μM Y27632 for 2 h. In all panels, asterisk (*) indicates p < 10^{-6}, N = 64–416 podosomes from four to five individual cells per bar. See numerical data in Supplemental Table 3.

those observed in WT OCLs (Figure 7 and Supplemental Table 3). The weaker effect of ROCK inhibition on podosomal life spans in WT OCLs in comparison to direct inhibition of Rho may be due to Rho acting via additional downstream effectors. The fact that inhibition of Rho corrected the podosomal stability phenotype of EKO osteoclasts leads us to conclude that Rho functions downstream of cyt-PTPe this respect. We note that the absolute life span of podosomal cores is affected also by the exact conditions the cells are grown in and, for example, ranged between 88 and 116 s for SZL podosomes in WT OCLs and between 113 and 212 s for similar podosomes in EKO OCLs. Nevertheless, in each experiment podosomes of WT OCLs were always clearly and significantly shorter lived than podosomes of EKO OCLs that were organized in the same type of structure (Figures 1, 6, and 7 and Supplemental Tables 1–3).

DISCUSSION

In this study, we present cellular and molecular data that show that cyt-PTPe is required for regulating the structure, organization, and dynamics of podosomes in osteoclasts. In the absence of this phosphatase, the structure of podosomes as punctate objects with an actin-rich core and their organization into an SZL at the cell periphery are severely disrupted. Lack of cyt-PTPe also prevents shortening of the life span of podosomal actin cores as they become part of rings and of the SZL. These results indicate that cyt-PTPe contributes to the normal destabilization of podosomes that occurs as the OCLs they reside in become functional. The well-established links between the organization of podosomes in osteoclasts and the ability of these cells to degrade bone strongly suggest that these podosomal abnormalities cause the reduced adhesion of osteoclasts to bone and reduced bone resorption in vitro and in vivo, which were described previously in EKO mice (Chiusaroli et al., 2004).

Adhesion of osteoclasts and organization of their podosomes are ultimately regulated by integrins (e.g., McHugh et al., 2000), which suggests that cyt-PTPe participates in integrin signaling in OCLs. The present study establishes that

integrin activation induces phosphorylation of cyt-PTPe exclusively at its C-terminal residue Y638 (Figure 4). The functional consequences of this phosphorylation event are significant and include enabling cyt-PTPe to associate with Src, to further activate this kinase and to shorten the life span of podosomal cores (Figure 6). The approximate twofold increase in Src activity in EKO OCLs upon cyt-PTPe expression (Figure 6B) is physiologically relevant because Src activity is reduced by approximately half in EKO OCLs (Figure 2A). Expression of cyt-PTPe in these cells then increases Src activity to levels found in WT OCLs and generates a clear physiological effect by altering podosomal stability (Figure 6F). Furthermore, the magnitude of this increase in Src activity is similar to that observed when RPTPe activates Src in fibroblasts and in mouse mammary tumor cells induced by Neu, in which it affects cellular morphology (Gil-Henn and Elson, 2003; Berman-Golan and Elson, 2007). C-Terminal phosphorylation does not seem to alter the specific activity of PTPe (Berman-Golan and Elson, 2007); its effect may be mediated by affecting the ability of PTPe to bind other molecules. The latter suggestion is consistent with the phospho-displacement model (Zheng et al., 2000), according to which the phosphorylated C-terminal of PTPe binds the SH2 domain of Src, thereby displacing pY527 of the kinase and promoting its dephosphorylation. The findings that cyt-PTPe must be phosphorylated to activate Src in osteoclasts and that this phosphorylation is induced after activation of integrins suggest that cyt-PTPe participates in linking Src activation with integrins. This conclusion is supported also by the finding that the stability of podosomes, which are highly responsive to integrin signaling, can be rescued in EKO OCLs by expressing cyt-PTPe, by expressing Src, or by inhibiting the downstream Src effector molecule Rho. It is important to note that lack of PTPe reduces, but does not abolish, activity of Src (Figure 6B; Gil-Henn and Elson, 2003; Berman-Golan and Elson, 2007) because other PTPs, such as PTP alpha (Zheng et al., 2000) and PTP-oc (Lau et al., 2006; Sheng et al., 2009) can activate Src. The exogenous Src added to EKO OCLs is therefore active.

Phosphorylation of cyt-PTPe subsequent to integrin activation is mediated at least in part by Src itself. Accordingly, phosphorylation of cyt-PTPe is increased when exogenous Src is added to cells and is decreased when Src is inhibited (Figure 5). Importantly, catalytic activity of cyt-PTPe is required for its own phosphorylation; this requirement can be overcome by constitutively active Src, whose activity is independent of cyt-PTPe. Collectively, these data suggest that cyt-PTPe participates in integrin signaling both upstream and downstream of Src and serves as a molecular amplifier of Src activity. According to this model (Figure 8), integrin activation partially activates Src. Src then induces phosphorylation of cyt-PTPe at Y638, either directly or indirectly; pY638 cyt-PTPe further activates the kinase, which affects podosomes by regulating Rho and other downstream effectors, such as ROCK. Because phosphorylation of cyt-PTPe at Y638 is critical for the above-mentioned activities, C-terminal dephosphorylation of cyt-PTPe may shut down the ability of cyt-PTPe affect integrin–Src–podosome signaling in OCLs. PTPe undergoes potent autodephosphorylation at its C-terminal tyrosine (Berman-Golan and Elson, 2007), suggesting a mechanism by which this may occur.

How is Src activated before phosphorylation of cyt-PTPe? Src can be activated by binding of the β3 subunit of αvβ3 integrin to the Src SH3 domain (Obergfell et al., 2002; Arias-Salgado et al., 2003). In addition, interaction between phospho-Y402 of Pyk2 and the Src SH2 domain counters the
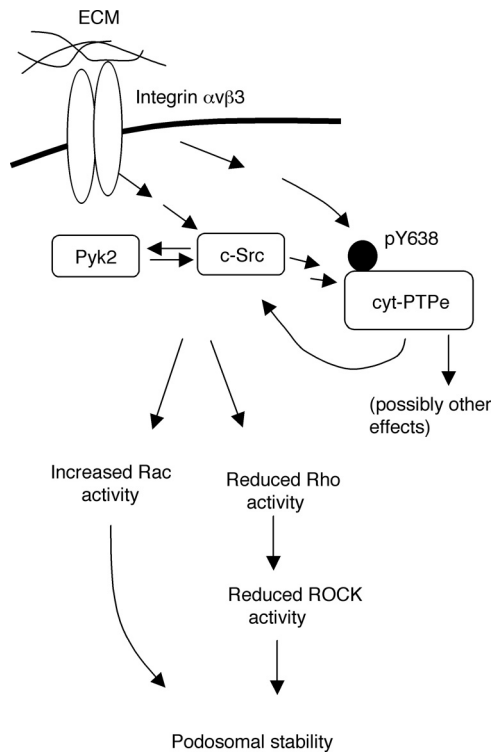
Figure 8. Schematic model suggesting how cyt-PTPe participates in activation of Src downstream of activated integrins in osteoclasts. Activation of integrins results in partial activation of Src by mechanisms that do not include cyt-PTPe as discussed. Src then participates in phosphorylation of cyt-PTPe at Y638; pY638 cyt-PTPe activates Src further, ensuring Src is sufficiently active to perform downstream roles, leading ultimately to normal stability of podosomes.

inhibitory intramolecular interaction between the SH2 domain and pY527 of Src (Lakkakorpi *et al.*, 2003; Horne *et al.*, 2005); phospholipase Cγ has also been suggested to link integrins with Src (Epple *et al.*, 2008). Src may also be partially activated by other PTPs in OCLs in a phosphorylation-independent manner. The related receptor-type PTP alpha (RPTPα) may fulfill such a role because it is expressed in OCLs (Chiusaroli *et al.*, 2004) and is reported to activate Src/Fyn downstream of integrins in fibroblasts in a manner that is independent of C-terminal phosphorylation (von Wichert *et al.*, 2003; Zeng *et al.*, 2003; Chen *et al.*, 2006; Abreu *et al.*, 2008). The respective roles of cyt-PTPe and RPTPα in integrin signaling may then differ in their timing: RPTPα may contribute to activation of Src initially upon integrin activation, whereas cyt-PTPe may participate in subsequent amplification and maintenance of Src activity. These distinct roles may arise from RPTPα being an integral receptor-type protein; cyt-PTPe is predominantly cytosolic and associates with the cell membrane only in part (Elson and Leder, 1995a). This single distinction accounts for the different modes of functional interaction between either phosphatase and the delayed rectifier, voltage-gated potassium channel Kv2.1 (Tiran *et al.*, 2006). One role of cyt-PTPe in osteoclasts is then to amplify activation of Src by integrins, which occurs initially via mechanisms that do not require cyt-PTPe.

Our results agree with those of Destaing *et al.* (2008), who showed that Src regulates the formation, structure, life span, and rate of actin polymerization in podosomes of primary OCLs. The kinase activity and either the SH2 or SH3 domains of Src are required to restore normal podosome organization and dynamics in Src-deficient OCLs (Destaing *et al.*, 2008); this last issue has not been addressed in EKO cells. The association between lack of cyt-PTPe, decreased Src activity and increased Rho activity also agrees with studies that document a Src-dependent decrease in Rho activity upon integrin activation (Arthur *et al.*, 2000). Reduced Src activity in the absence of cyt-PTPe should then prevent the expected reduction in Rho activity, as we have observed. The functional significance of the reductions observed in Pyk2 phosphorylation and Rac activity in EKO OCLs remain to be determined.

Nevertheless, Src and Pyk2 associate with each other in OCLs, and both kinases are pulled down with cyt-PTPe in these cells (Figure 6E). We believe Src is the main partner of cyt-PTPe in this system because Src is significantly more effective than Pyk2 in inducing phosphorylation of cyt-PTPe (Figure 5A) and because, in contrast with Pyk2, Src is activated by tyrosine dephosphorylation. Because Src can phosphorylate Pyk2 in OCLs, reduced phosphorylation of Pyk2 in EKO OCLs (Figure 2B) may be an indirect consequence of reduced Src activity in the absence of cyt-PTPe. Further studies are required to determine whether cyt-PTPe can regulate Pyk2 directly.

Our findings concerning the small GTPases Rho and Rac agree with the established roles of these molecules in regulating podosomes in osteoclasts downstream of integrin activation (Zhang *et al.*, 1995; Chellaiah *et al.*, 2000; Ory *et al.*, 2000, 2008; Fukuda *et al.*, 2005). Increased Rho activity destabilizes the SZL in OCLs (Ory *et al.*, 2008), whereas inhibition of Rho stabilizes the SZL in correlation with acetylation and stabilization of the microtubule network in these cells (Destaing *et al.*, 2005). In agreement, OCLs from mice lacking Pyk2 exhibit increased Rho activity, reduced stability of the SZL, and reduced microtubule acetylation (Gil-Henn *et al.*, 2007). Acetylation of tubulin is not reduced in EKO OCLs (data not shown), possibly because these cells are not null for Pyk2. Rac and Rho perform antagonistic functions in several systems, including cytoskeletal organization in neurite formation (Leeuwen *et al.*, 1997), Swiss 3T3 cells (Rottner *et al.*, 1999), and avian multinucleated cells (Ory *et al.*, 2000, 2002), in correlation with the opposite effects lack of cyt-PTPe has on both proteins in OCLs.

Finally, other PTPs activate Src in various physiological systems, and some PTPs have been shown to activate Src in OCLs (Yang *et al.*, 2007; Shivtiel *et al.*, 2008); activation of Src in OCLs is then not the exclusive domain of cyt-PTPe. Nevertheless, the existence of a clear integrin-related podosomal phenotype in EKO osteoclasts indicates that cyt-PTPe plays a role that cannot be compensated for by other PTPs. cyt-PTPe may play a qualitatively unique role, for example, by acting in a unique signaling context, or its contribution to the total PTP activity that targets Src may be significant enough such that its absence reduces Src activity below a minimal threshold needed for proper cellular function. In view of the central role integrins play in many diverse cell types and because the receptor-type form of PTPe is also responsive to integrin signaling, PTPe may participate in integrin signaling in additional cell types as well.

ACKNOWLEDGMENTS

REFERENCES

Abreu, M. T., Penton, P. C., Kwok, V., Vachon, E., Shalloway, D., Vidali, L., Lee, W., McCulloch, C. A., and Downey, G. P. (2008). Tyrosine phosphatase PTPalpha regulates focal adhesion remodeling through Rac1 activation. Am. J. Physiol. Cell Physiol. *294*, C931–C944.

Amoui, M., Sheng, M. H., Chen, S. T., Baylink, D. J., and Lau, K. H. (2007). A transmembrane osteoclastic protein-tyrosine phosphatase regulates osteoclast activity in part by promoting osteoclast survival through c-Src-dependent activation of NFkappaB and JNK2. Arch. Biochem. Biophys. *463*, 47–59.

Aoki, K., Didomenico, E., Sims, N. A., Mukhopadhyay, K., Neff, L., Houghton, A., Amling, M., Levy, J. B., Horne, W. C., and Baron, R. (1999). The tyrosine phosphatase SHP-1 is a negative regulator of osteoclastogenesis and osteoclast resorbing activity: increased resorption and osteopenia in me(v)/me(v) mutant mice. Bone *25*, 261–267.

Arias-Salgado, E. G., Lizano, S., Sarkar, S., Brugge, J. S., Ginsberg, M. H., and Shattil, S. J. (2003). Src kinase activation by direct interaction with the integrin beta cytoplasmic domain. Proc. Natl. Acad. Sci. USA. *100*, 13298–13302.

Arthur, W. T., Petch, L. A., and Burridge, K. (2000). Integrin engagement suppresses RhoA activity via a c-Src-dependent mechanism. Curr. Biol. *10*, 719–722.

Berman-Golan, D., and Elson, A. (2007). Neu-mediated phosphorylation of protein tyrosine phosphatase epsilon is critical for activation of Src in mammary tumor cells. Oncogene *26*, 7028–7037.

Bruzzaniti, A., and Baron, R. (2006). Molecular regulation of osteoclast activity. Rev. Endocr. Metab. Disord. *7*, 123–139.

Chellaiah, M. A., and Schaller, M. D. (2009). Activation of Src kinase by protein-tyrosine phosphatase-PEST in osteoclasts: comparative analysis of the effects of bisphosphonate and protein-tyrosine phosphatase inhibitor on Src activation in vitro. J. Cell. Physiol. *220*, 382–393

Chellaiah, M. A., Soga, N., Swanson, S., McAllister, S., Alvarez, U., Wang, D., Dowdy, S. F., and Hruska, K. A. (2000). Rho-A is critical for osteoclast podosome organization, motility, and bone resorption. J. Biol. Chem. *275*, 11993–12002.

Chen, M., Chen, S. C., and Pallen, C. J. (2006). Integrin-induced tyrosine phosphorylation of protein-tyrosine phosphatase-alpha is required for cytoskeletal reorganization and cell migration. J. Biol. Chem. *281*, 11972–11980.

Chiusaroli, R., Knobler, H., Luxenburg, C., Sanjay, A., Granot-Attas, S., Tiran, Z., Miyazaki, T., Harmelin, A., Baron, R., and Elson, A. (2004). Tyrosine phosphatase epsilon is a positive regulator of osteoclast function in vitro and in vivo. Mol. Biol. Cell *15*, 234–244.

Destaing, O., Saltel, F., Geminard, J. C., Jurdic, P., and Bard, F. (2003). Podosomes display actin turnover and dynamic self-organization in osteoclasts expressing actin-green fluorescent protein. Mol. Biol. Cell *14*, 407–416.

Destaing, O., Saltel, F., Gilquin, B., Chabadel, A., Khochbin, S., Ory, S., and Jurdic, P. (2005). A novel Rho-mDia2-HDAC6 pathway controls podosome patterning through microtubule acetylation in osteoclasts. J. Cell Sci. *118*, 2901–2911.

Destaing, O., Sanjay, A., Itzstein, C., Horne, W. C., Toomre, D., De Camilli, P., and Baron, R. (2008). The tyrosine kinase activity of c-Src regulates actin dynamics and organization of podosomes in osteoclasts. Mol. Biol. Cell *19*, 394–404.

Elson, A., and Leder, P. (1995a). Identification of a cytoplasmic, phorbol ester-inducible isoform of protein tyrosine phosphatase epsilon. Proc. Natl. Acad. Sci. USA *92*, 12235–12239.

Elson, A., and Leder, P. (1995b). Protein-tyrosine phosphatase epsilon. An isoform specifically expressed in mouse mammary tumors initiated by v-Ha-ras OR neu. J. Biol. Chem. *270*, 26116–26122.

Epple, H., Cremasco, V., Zhang, K., Mao, D., Longmore, G. D., and Faccio, R. (2008). Phospholipase Cgamma2 modulates integrin signaling in the osteoclast by affecting the localization and activation of Src kinase. Mol. Cell Biol. *28*, 3610–3622.

Fischer, M., Kaech, S., Wagner, U., Brinkhaus, H., and Matus, A. (2000). Glutamate receptors regulate actin-based plasticity in dendritic spines. Nat. Neurosci. *3*, 887–894.

Flint, A. J., Tiganis, T., Barford, D., and Tonks, N. K. (1997). Development of "substrate-trapping" mutants to identify physiological substrates of protein tyrosine phosphatases. Proc. Natl. Acad. Sci. USA *94*, 1680–1685.

Fukuda, A., Hikita, A., Wakeyama, H., Akiyama, T., Oda, H., Nakamura, K., and Tanaka, S. (2005). Regulation of osteoclast apoptosis and motility by small GTPase binding protein Rac1. J. Bone Miner. Res. *20*, 2245–2253.

Geiger, B., Bershadsky, A., Pankov, R., and Yamada, K. M. (2001). Transmembrane crosstalk between the extracellular matrix–cytoskeleton crosstalk. Nat. Rev. Mol. Cell Biol. *2*, 793–805.

Gil-Henn, H., Destaing, O., Sims, N. A., Aoki, K., Alles, N., Neff, L., Sanjay, A., Bruzzaniti, A., De Camilli, P., Baron, R., and Schlessinger, J. (2007). Defective microtubule-dependent podosome organization in osteoclasts leads to increased bone density in Pyk2/mice. J. Cell Biol. *178*, 1053–1064.

Gil-Henn, H., and Elson, A. (2003). Tyrosine phosphatase-epsilon activates Src and supports the transformed phenotype of Neu-induced mammary tumor cells. J. Biol. Chem. *278*, 15579–15586.

Gil-Henn, H., Volohonsky, G., Toledano-Katchalski, H., Gandre, S., and Elson, A. (2000). Generation of novel cytoplasmic forms of protein tyrosine phosphatase epsilon by proteolytic processing and translational control. Oncogene *19*, 4375–4384.

Gimona, M. (2008). The microfilament system in the formation of invasive adhesions. Semin. Cancer Biol. *18*, 23–34.

Gimona, M., and Buccione, R. (2006). Adhesions that mediate invasion. Int. J. Biochem. Cell Biol. *38*, 1875–1892.

Gimona, M., Buccione, R., Courtneidge, S. A., and Linder, S. (2008). Assembly and biological role of podosomes and invadopodia. Curr. Opin. Cell Biol. *20*, 235–241.

Granot-Attas, S., and Elson, A. (2008). Protein tyrosine phosphatases in osteoclast differentiation, adhesion, and bone resorption. Eur. J. Cell Biol. *87*, 479–490.

Horne, W. C., Sanjay, A., Bruzzaniti, A., and Baron, R. (2005). The role(s) of Src kinase and Cbl proteins in the regulation of osteoclast differentiation and function. Immunol. Rev. *208*, 106–125.

Jurdic, P., Saltel, F., Chabadel, A., and Destaing, O. (2006). Podosome and sealing zone: specificity of the osteoclast model. Eur. J. Cell Biol. *85*, 195–202.

Kollet, O., et al. (2006). Osteoclasts degrade endosteal components and promote mobilization of hematopoietic progenitor cells. Nat. Med. *12*, 657–664.

Kraut, J., Volohonsky, G., Toledano-Katchalski, H., and Elson, A. (2002). Nuclear localization of non-receptor protein tyrosine phosphatase epsilon is regulated by its unique N-terminal domain. Exp. Cell Res. *281*, 182–189.

Krueger, N. X., Streuli, M., and Saito, H. (1990). Structural diversity and evolution of human receptor-like protein tyrosine phosphatases. EMBO J. *9*, 3241–3252.

Lakkakorpi, P. T., Bett, A. J., Lipfert, L., Rodan, G. A., and Duong le, T. (2003). PYK2 autophosphorylation, but not kinase activity, is necessary for adhesion-induced association with c-Src, osteoclast spreading, and bone resorption. J. Biol. Chem. *278*, 11502–11512.

Lau, K. H., Wu, L. W., Sheng, M. H., Amoui, M., Suhr, S. M., and Baylink, D. J. (2006). An osteoclastic protein-tyrosine phosphatase is a potential positive regulator of the c-Src protein-tyrosine kinase activity: a mediator of osteoclast activity. J. Cell Biochem. *97*, 940–955.

Leeuwen, F. N., Kain, H. E., Kammen, R. A., Michiels, F., Kranenburg, O. W., and Collard, J. G. (1997). The guanine nucleotide exchange factor Tiam1 affects neuronal morphology; opposing roles for the small GTPases Rac and Rho. J. Cell Biol. *139*, 797–807.

Linder, S. (2007). The matrix corroded: podosomes and invadopodia in extracellular matrix degradation. Trends Cell Biol. *17*, 107–117.

Linder, S., and Aepfelbacher, M. (2003). Podosomes: adhesion hot-spots of invasive cells. Trends Cell Biol. *13*, 376–385.

Lowe, C., Yoneda, T., Boyce, B. F., Chen, H., Mundy, G. R., and Soriano, P. (1993). Osteopetrosis in Src-deficient mice is due to an autonomous defect of osteoclasts. Proc. Natl. Acad. Sci. USA *90*, 4485–4489.

Luxenburg, C., Addadi, L., and Geiger, B. (2006a). The molecular dynamics of osteoclast adhesions. Eur. J. Cell Biol. *85*, 203–211.

Luxenburg, C., Geblinger, D., Klein, E., Anderson, K., Hanein, D., Geiger, B., and Addadi, L. (2007). The architecture of the adhesive apparatus of cultured osteoclasts: from podosome formation to sealing zone assembly. PLoS ONE *2*, e179.

Luxenburg, C., Parsons, J. T., Addadi, L., and Geiger, B. (2006b). Involvement of the Src-cortactin pathway in podosome formation and turnover during polarization of cultured osteoclasts. J. Cell Sci. *119*, 4878–4888.

McHugh, K. P., Hodivala-Dilke, K., Zheng, M. H., Namba, N., Lam, J., Novack, D., Feng, X., Ross, F. P., Hynes, R. O., and Teitelbaum, S. L. (2000). Mice lacking beta3 integrins are osteosclerotic because of dysfunctional osteoclasts. J. Clin. Invest. *105*, 433–440.

Miyazaki, T., Sanjay, A., Neff, L., Tanaka, S., Horne, W. C., and Baron, R. (2004). SRC kinase activity is essential for osteoclast function. J. Biol. Chem. *279*, 17660–17666.

Obergfell, A., Eto, K., Mocsai, A., Buensuceso, C., Moores, S. L., Brugge, J. S., Lowell, C. A., and Shattil, S. J. (2002). Coordinate interactions of Csk, Src, and Syk kinases with αIIbβ3 initiate integrin signaling to the cytoskeleton. J. Cell Biol. *157*, 265–275.

Ory, S., Brazier, H., Pawlak, G., and Blangy, A. (2008). Rho GTPases in osteoclasts: Orchestrators of podosome arrangement. Eur. J. Cell Biol. *87*, 469–477.

Ory, S., Destaing, O., and Jurdic, P. (2002). Microtubule dynamics differentially regulates Rho and Rac activity and triggers Rho-independent stress fiber formation in macrophage polykaryons. Eur. J. Cell Biol. *81*, 351–362.

Ory, S., Munari-Silem, Y., Fort, P., and Jurdic, P. (2000). Rho and Rac exert antagonistic functions on spreading of macrophage-derived multinucleated cells and are not required for actin fiber formation. J. Cell Sci. *113*, 1177–1188.

Peretz, A., Gil-Henn, H., Sobko, A., Shinder, V., Attali, B., and Elson, A. (2000). Hypomyelination and increased activity of voltage-gated K(+) channels in mice lacking protein tyrosine phosphatase epsilon. EMBO J. *19*, 4036–4045.

Ross, F. P. (2006). M-CSF, c-Fms, and signaling in osteoclasts and their precursors. Ann. N.Y. Acad. Sci. *1068*, 110–116.

Rottner, K., Hall, A., and Small, J. V. (1999). Interplay between Rac and Rho in the control of substrate contact dynamics. Curr. Biol. *9*, 640–648.

Saltel, F., Chabadel, A., Bonnelye, E., and Jurdic, P. (2008). Actin cytoskeletal organisation in osteoclasts: a model to decipher transmigration and matrix degradation. Eur. J. Cell Biol. *87*, 459–468.

Sanjay, A., *et al*. (2001). Cbl associates with Pyk2 and Src to regulate Src kinase activity, alpha(v)beta(3) integrin-mediated signaling, cell adhesion, and osteoclast motility. J. Cell Biol. *152*, 181–195.

Schwartzberg, P. L., Xing, L., Hoffmann, O., Lowell, C. A., Garrett, L., Boyce, B. F., and Varmus, H. E. (1997). Rescue of osteoclast function by transgenic expression of kinase-deficient Src in src−/− mutant mice. Genes Dev. *11*, 2835–2844.

Sheng, M. H., Amoui, M., Stiffel, V., Srivastava, A. K., Wergedal, J. E., and Lau, K. H. (2009). Targeted transgenic expression of an osteoclastic transmembrane protein-tyrosine phosphatase in cells of osteoclastic lineage increases bone resorption and bone loss in male young adult mice. J. Biol. Chem. *284*, 11531–11545.

Shivtiel, S., *et al*. (2008). CD45 regulates retention, motility, and numbers of hematopoietic progenitors, and affects osteoclast remodeling of metaphyseal trabecules. J. Exp. Med. *205*, 2381–2395.

Sines, T., Granot-Attas, S., Weisman-Welcher, S., and Elson, A. (2007). Association of tyrosine phosphatase epsilon with microtubules inhibits phosphatase activity and is regulated by the epidermal growth factor receptor. Mol. Cell Biol. *27*, 7102–7112.

Soriano, P., Montgomery, C., Geske, R., and Bradley, A. (1991). Targeted disruption of the c-src proto-oncogene leads to osteopetrosis in mice. Cell *64*, 693–702.

Tanaka, S., Amling, M., Neff, L., Peyman, A., Uhlmann, E., Levy, J. B., and Baron, R. (1996). c-Cbl is downstream of c-Src in a signalling pathway necessary for bone resorption. Nature *383*, 528–531.

Tanuma, N., Nakamura, K., and Kikuchi, K. (1999). Distinct promoters control transmembrane and cytosolic protein tyrosine phosphatase epsilon expression during macrophage differentiation. Eur. J. Biochem. *259*, 46–54.

Teitelbaum, S. L. (2007). Osteoclasts: what do they do and how do they do it? Am. J. Pathol. *170*, 427–435.

Tiran, Z., Peretz, A., Sines, T., Shinder, V., Sap, J., Attali, B., and Elson, A. (2006). Tyrosine phosphatases epsilon and alpha perform specific and overlapping functions in regulation of voltage-gated potassium channels in Schwann cells. Mol. Biol. Cell *17*, 4330–4342.

Toledano-Katchalski, H., and Elson, A. (1999). The transmembranal and cytoplasmic forms of protein tyrosine phosphatase epsilon physically associate with the adaptor molecule Grb2. Oncogene *18*, 5024–5031.

Umeda, S., Beamer, W. G., Takagi, K., Naito, M., Hayashi, S., Yonemitsu, H., Yi, T., and Shultz, L. D. (1999). Deficiency of SHP-1 protein-tyrosine phosphatase activity results in heightened osteoclast function and decreased bone density. Am. J. Pathol. *155*, 223–233.

von Wichert, G., Jiang, G., Kostic, A., De Vos, K., Sap, J., and Sheetz, M. P. (2003). RPTP-alpha acts as a transducer of mechanical force on alphav/beta3-integrin-cytoskeleton linkages. J. Cell Biol. *161*, 143–153.

Wada, T., Nakashima, T., Hiroshi, N., and Penninger, J. M. (2006). RANKL-RANK signaling in osteoclastogenesis and bone disease. Trends Mol. Med. *12*, 17–25.

Yang, J. H., Amoui, M., and Lau, K. H. (2007). Targeted deletion of the osteoclast protein-tyrosine phosphatase (PTP-oc) promoter prevents RANKL-mediated osteoclastic differentiation of RAW264.7 cells. FEBS Lett. *581*, 2503–2508.

Zeng, L., Si, X., Yu, W. P., Le, H. T., Ng, K. P., Teng, R. M., Ryan, K., Wang, D. Z., Ponniah, S., and Pallen, C. J. (2003). PTP alpha regulates integrin-stimulated FAK autophosphorylation and cytoskeletal rearrangement in cell spreading and migration. J. Cell Biol. *160*, 137–146.

Zhang, D., *et al*. (1995). The small GTP-binding protein, rho p21, is involved in bone resorption by regulating cytoskeletal organization in osteoclasts. J. Cell Sci. *108*, 2285–2292.

Zhang, Z., Jimi, E., and Bothwell, A. L. (2003). Receptor activator of NF-kappa B ligand stimulates recruitment of SHP-1 to the complex containing TNFR-associated factor 6 that regulates osteoclastogenesis. J. Immunol. *171*, 3620–3626.

Zheng, X. M., Resnick, R. J., and Shalloway, D. (2000). A phosphotyrosine displacement mechanism for activation of Src by PTPalpha. EMBO J. *19*, 964–978.

Zou, W., Kitaura, H., Reeve, J., Long, F., Tybulewicz, V. L., Shattil, S. J., Ginsberg, M. H., Ross, F. P., and Teitelbaum, S. L. (2007). Syk, c-Src, the alphavbeta3 integrin, and ITAM immunoreceptors, in concert, regulate osteoclastic bone resorption. J. Cell Biol. *176*, 877–888.